

Characterization of excited states of ultracold atoms in optical lattices

Mateusz Łącki,¹ Dominique Delande,² and Jakub Zakrzewski^{1,3}

¹ *Instytut Fizyki imienia Mariana Smoluchowskiego,*

Uniwersytet Jagielloński, ulica Reymonta 4, PL-30-059 Kraków, Poland

² *Laboratoire Kastler-Brossel, UPMC-Paris 6, ENS, CNRS; 4 Place Jussieu, F-75005 Paris, France*

³ *Mark Kac Complex Systems Research Center, Uniwersytet Jagielloński, Kraków, Poland*

(Dated: June 27, 2011)

Loading ultracold atoms in an optical lattice from a Bose-Einstein condensate is generally a non-adiabatic process resulting in the dynamical excitation of a wavepacket, a combination of several eigenstates. Using the time evolving block decimation algorithm, we show how to extract information on these excited states, and how their properties differ from those of the ground state. This allows for a deeper understanding of nonadiabaticity in experimental realizations of insulating phases.

PACS numbers: 67.85.Hj, 03.75.Kk, 03.75.Lm

The seminal suggestion of Jaksch and Zoller [1] to realize the Bose-Hubbard (BH) model [2] in a gas of ultra cold atoms in an optical lattice was soon followed by the observation of a quantum phase transition (QPT) from a superfluid (SF) phase to a Mott insulator (MI) [3]. This experiment, showing the unique control of system parameters in cold atomic gases, opened up the possibility of studying experimentally many-body systems in the presence of interaction and external perturbations, for a review see [4]. Of special interest is the addition of an external disordered potential, where a new phase - insulating, compressible and gapless - named Bose glass (BG), has been predicted [2]. Experimental results available are compatible with the existence of such a phase [5, 6], but not fully conclusive: the system is prepared from a low temperature Bose-Einstein condensate by ramping up an optical lattice, starting from a SF initial state; preparing a MI or a BG requires to go through a QPT, which is known in general to be non adiabatic [7, 8], i.e. to create some excitations in the system.

A mean field simulation [9] of the experiment [3] suggested significant excitation of the system. For systems of reduced dimensionality [5], calculations beyond mean field approximation show that the breakdown of adiabaticity across the SF-MI transition is quite important [10], the prepared state having only 10% overlap with the ground MI state.

The situation is even worse for the disordered system. Disorder leads to a complicated energy levels structure with many states lying close to the ground state. In effect the adiabaticity is completely lost when the disorder is turned on, both for shallow [11] and deep [10] lattices.

It seems important, therefore, to understand the properties of excited states that are significantly populated as well as how they combine into the dynamically created wavepacket. It was suggested that, deep in the Mott regime, these states are MI with defects [12]. This has been partially confirmed experimentally via direct imaging of atoms in optical lattices [13]. Still direct theoretical evidence seems necessary. This is the aim of the present

work. We show that it is possible to construct the excited states from the dynamically evolved state in this many-body interacting system. We take as a case example the Florence experiment [5], although the methods can be extended to other systems.

The main features of the experiment are as follows (for details see [5]). A ⁸⁷Rb condensate in a harmonic trap is loaded in a deep two dimensional optical lattice potential (the “transverse lattice”) realizing an array of one-dimensional (1D) atomic tubes. While ramping up the transverse lattice, an optical potential along the tubes is ramped up as well. This may be either a regular optical lattice only or a combination of two incommensurate standing waves realizing a quasi-disorder [5]. The natural energy scale in the problem is the recoil energy $E_R = \hbar^2/2m\lambda^2$ where λ is the wavelength of lasers forming the optical lattice and m the atomic mass. The optical potential from a pair of counter propagating beams is then $V/E_R = s \sin^2(2\pi x/\lambda)$. In the experiment, $\lambda = 830\text{nm}$ while the maximal depth “along” the tubes is $s = 14$ deep in the Mott regime (the SF-MI transition appears around $s=8-9$ [10]). When all lattices are ramped up, soon the tubes become isolated, making the dynamics effectively 1D. Along the relevant direction, the standing wave creates a periodic lattice. Following [1] we can use a Bose-Hubbard Hamiltonian [20]:

$$H = -J \sum_{\langle j, j' \rangle} b_j^\dagger b_{j+1} + \frac{U}{2} \sum_j n_j (n_j - 1) + \sum_j \epsilon_j n_j, \quad (1)$$

where b_j (b_j^\dagger) is the destruction (creation) operator of one particle at the j -th site, $n_j = b_j^\dagger b_j$ the particle number operator, and $\langle j, j' \rangle$ indicates the sum over nearest neighbors only. The tunneling rate J and the interaction energy U can be found as appropriate integrals of Wannier functions [1]. When this depth is changed in time, J and U become time-dependent. ϵ_j represents the energy offset at a given site, due to the harmonic trap and, if present, to the additional lattice producing the

quasi-disorder:

$$\epsilon_j = \frac{m\omega^2 a^2}{2}(j - r_0)^2 + s_2 E_{R2} \sin^2 \left(\frac{\pi j \lambda}{\lambda_2} + \phi \right). \quad (2)$$

Here ω is the (time-dependent due to transverse lattice profile [5]) trapping frequency, r_0 the minimum of the trap, a the lattice constant, $\lambda_2 = 1076\text{nm}$ the wavelength of the second laser, s_2 the amplitude (in recoil energy units for λ_2) of the quasi-disorder, and ϕ its phase.

As described in [10], we start the time evolution from the ground state at $s = 4$. We integrate numerically the evolution of the system when s increases using the Time Evolving Block Decimation (TEBD) algorithm [14]. At different lattice depths s , we calculate the overlap of the dynamically evolved wave packet on the ground state for that s (obtained by imaginary time propagation method using the same TEBD algorithm). For adiabatic evolution the overlap should stay close to unity. We observed its reduction in the region of the SF-MI transition [10].

A partial analysis of the dynamically created wave packet has been carried out in [10]. For that purpose we evolved the wavepacket at a *constant* final s value for some time and calculated its autocorrelation function. The evolution of a state by a time-independent Hamiltonian with eigenbasis $|e_i\rangle$ is given by $|\psi(t)\rangle = \sum_i \exp(-iE_i t/\hbar) c_i |e_i\rangle$. The eigenstates $|e_i\rangle$ and eigenenergies E_i are not known, except for the ground state. The Fourier transform (FT) of the autocorrelation function $C(t) = \langle \psi(0) | \psi(t) \rangle = \sum_i |c_i|^2 \exp(-iE_i t/\hbar)$ over a time interval T is the autocorrelation spectrum:

$$\tilde{C}_T(E) = \frac{1}{T} \int_{-T/2}^{T/2} e^{\frac{iEt}{\hbar}} C(t) dt = \sum_i |c_i|^2 \text{sinc} \frac{(E - E_i)T}{2\hbar} \quad (3)$$

where $\text{sinc } x = \sin x/x$. In the limit of long time T , it yields narrow peaks at the E_i 's with weights $|c_i|^2$ [10]. Here we extend this analysis extracting also the excited eigenstates with large overlap - those contribute most to the dynamical wavepacket. We perform a FT *directly* on $|\psi(t)\rangle$:

$$|\phi_T(E)\rangle = \frac{1}{T} \int_{-T/2}^{T/2} e^{\frac{iEt}{\hbar}} |\psi(t)\rangle dt = \sum_i c_i \text{sinc} \frac{(E - E_i)T}{2\hbar} |e_i\rangle \quad (4)$$

For long T , $|\phi_T(E_i)\rangle \rightarrow c_i |e_i\rangle$, providing us with the targeted eigenstate. Importantly, the method selects excited states *relevant for the dynamics*, although there may be in the same spectral region myriads of other eigenstates.

The details of this procedure performed in the Matrix Product State (MPS) representation will be published elsewhere [15]. It is sufficient to say that the TEBD algorithm produces the $|\psi(t)\rangle$ on a discrete set of times, each one as a MPS, calculating the FT reduces to a series of MPS additions. As shown in [16], the sum of two MPSs is itself a MPS. In effect a stable and reliable algorithm for FT evaluation may be constructed [15].

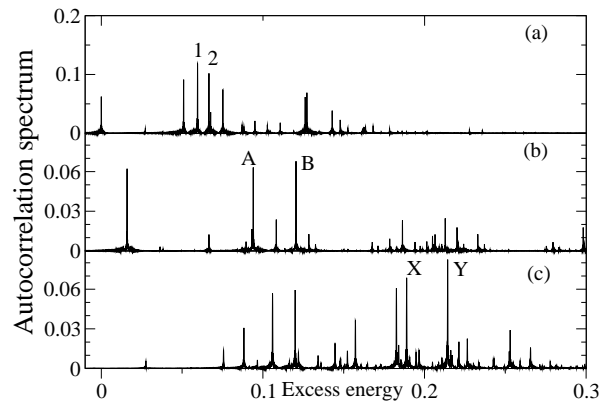


Figure 1: Autocorrelation spectra, Eq. (3), obtained dynamically for $s=14$ after switching on the optical lattice, for three increasing disorder strengths $s_2 =$ (a) 0, (b) 0.4375, (c) 2.1875. All parameters are taken as closely as possible to the experimental situation [5] (we use 151 atoms). The peaks appear at energy levels of the system (measured with respect to the ground state), with an intensity equal to the squared overlap with the wavepacket. The symbols in the plots denote excitations analysed in subsequent figures.

For a MPS, the calculation of average values of simple operators is easy and cheap [16]. This includes the average occupation number $\langle n_l \rangle$ at site l , its variance $\Delta_l = \sqrt{\langle n_l^2 \rangle - \langle n_l \rangle^2}$ and the correlation functions $\langle b_k b_l^\dagger \rangle$.

If we partition a system described by the density matrix ρ into two parts L (containing sites $1 \dots l$) and R (sites $l+1 \dots M$), the set of positive eigenvalues $(\lambda_\alpha^{[l]})^2$ of $\rho_L = \text{Tr}_R \rho$ forms the entanglement spectrum. It appears very naturally in the MPS representation [14]. The associated entanglement entropy is defined by

$$S_l = - \sum_\alpha (\lambda_\alpha^{[l]})^2 \ln (\lambda_\alpha^{[l]})^2 \quad (5)$$

and is important in e.g. studies of topological phases [17].

All such quantities can be easily computed for any state in MPS representation, be it the ground state, an excited state or a dynamically created wavepacket.

We now present the results. Fig. 1 shows the autocorrelation spectrum, eq. (3), of the dynamically created wavepacket evolved up to $s = 14$ using the experimental exponential ramp [5], at increasing disorder strengths.

In the absence of disorder ($s_2 = 0$), about ten states are significantly excited proving that the preparation is not really adiabatic. In fig. 2, we show various relevant quantities for the ground state, few excited states and the wavepacket. The average occupation number $\langle n_l \rangle$ on each site l has the well known “wedding cake” structure, with large MI regions with integer $\langle n_l \rangle$ separated by narrow SF regions. Because the energy excess brought by non adiabatic preparation is small, all significantly populated excited states have similar shapes. Clearly, all excitations take place in or around the SF regions: these are

transfers of one atom from the edge of a Mott plateau to the edge of another Mott plateau or to the neighboring SF region (“melting” of the Mott plateau). The standard excitations in an homogeneous system (without trapping potential) such as a particle-hole excitation in a Mott plateau are absent in the stationary excited states because they are dynamically unstable. They are also absent in the wavepacket because they are energetically too costly: a particle-hole excitation for a homogeneous system costs one interaction energy $U = 0.6$, much larger than the excess energy of the wavepacket 0.1. In particular, the description used in [12] where the ground state is contaminated by local particle-hole excitations is not compatible with our findings. A description in terms of melting of the MI [18] seems more relevant. For such a large s value, deep in the MI regime, it is in fact possible to identify and characterize quantitatively several low-energy excitations, and thus to label all the significantly populated states [15]. The variance of the occupation number Δ_l , confirms the existence of large MI regions with low Δ_l separated by SF peaks with larger Δ_l . While the ground state and excited states look very similar - except for small displacements of the SF regions - the wavepacket looks quite different, with higher Δ_l in the SF peaks. An even more dramatic difference is visible in the entanglement entropy. For the eigenstates, it is essentially zero in the MI regions - which is expected as the state is mainly a product of Fock states on each site - and displays sharp peaks in the SF regions. In stark contrast, the entanglement entropy of the wavepacket is non-zero everywhere, including in the Mott plateaus. This may have important experimental consequences: suppose one splits the system in two parts in the middle of a Mott plateau and measures the number of particles in one part. For the ground state, this number will be almost the same in every realization of the experiment; for the wavepacket, it will have much larger fluctuations. Thus, although excited states building the wavepacket can be called Mott insulators, this is not true for the wavepacket itself.

The presence of disorder strongly modifies the properties of the system. A detailed analysis of possible phases is available [19], both for a truly random disorder [2] and a quasi-random disorder due to the secondary laser. We show here exemplary excitations occurring in the presence of quasi-disorder (2). We consider both a small $s_2 = 0.4375$ and a large disorder $s_2 = 2.1875$ for which no MI phase exist and the ground state forms a BG.

The overlap of the wavepacket with the ground state at final $s = 14$ is negligibly small in both cases (the corresponding peak at the origin is absent in Fig. 1) and many excited states are populated with appreciable efficiency. Obviously, the breakdown of adiabaticity is stronger than in the absence of disorder, with a slightly larger excess of energy 0.18-0.2 and more states significantly excited.

The properties of various states are shown in figs. 3 and

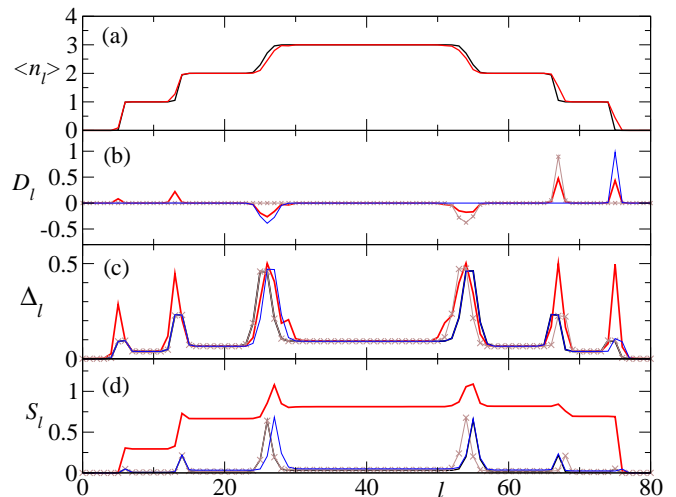


Figure 2: (color online) Properties of states of the Bose-Hubbard system in the deep Mott insulator phase ($s = 14$), in the absence of disorder ($s_2 = 0$), $r_0 = 0.12345$ in Eq. (2) being non integer to break the parity symmetry with respect to trap center. The black thin lines refer to the ground state, the red thick line to the dynamically prepared wavepacket, the brown (with crosses) and blue lines to the two excited states with the largest populations denoted as 1 and 2 in Fig. 1a. (a): Average occupation number $\langle n_l \rangle$ on each site, with the familiar wedding cake structure. (b): Difference $D_l = \langle n_l \rangle - \langle n_l \rangle_{\text{Ground state}}$ showing that the excitations take place around the SF regions, when atoms jump from a Mott plateau to another Mott plateau or to a SF region. (c): Variance $\Delta_l = \sqrt{\langle n_l^2 \rangle - \langle n_l \rangle^2}$. The peaks in the SF regions are significantly larger for the wavepacket than for stationary states. (d): Entanglement entropy, Eq. (5). While it is almost zero for the ground and excited states inside the Mott plateaus - implying approximate separability of the many-body state - it is large for the wavepacket.

4 for $s_2 = 0.4375$ and $s_2 = 2.1875$. For small s_2 , several MI phases - identified by plateaus in $\langle n_l \rangle$ - clearly continue to exist, separated by intermediate regions which can be either SF or a BG. Remarkably, the ground state and the excited states do have very similar structures, with several visible Mott plateaus. In contrast, these plateaus are less visible (only the central one seems to survive, with a reduced size) for the wavepacket. This can be interpreted as a partial melting of the BG and MI phases, producing a thermal insulator [18]. Note that the energy excess is still too small to create *local* particle-hole excitations which could travel across the system.

At $s_2 = 2.1875$, one does not expect the MI to survive [5, 19], the only insulating phase remaining being the BG. Exemplary excitations are shown in fig. 4. The occupations of various sites strongly fluctuate with disorder, low lying excitations seem in fact quite similar to the ground state. Excitations are *local* in character modifying the occupation number and its variance in selected sites only, and the entanglement entropy is small everywhere,

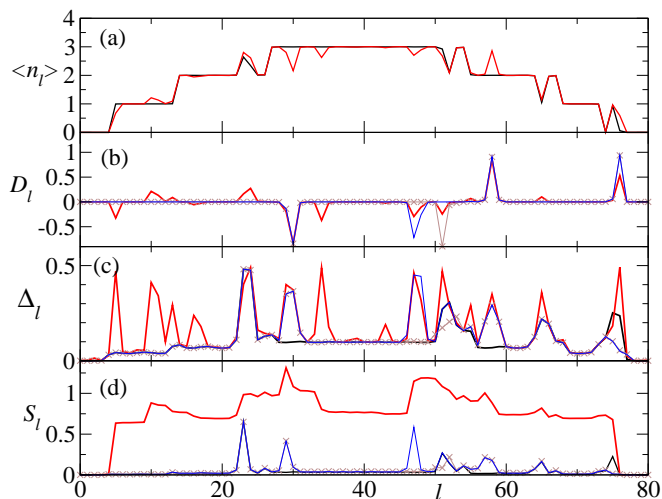


Figure 3: (color online) Same as fig. 2 but for small disorder ($s_2 = 0.4375$). Here $r_0 = 0$ and $\phi = 0.5432$ in Eq.(2). Brown (blue) lines correspond to excitations A and B indicated in the autocorrelation spectrum, Fig. 1(b). Mott insulating regions are clearly visible for the ground state and the excited states, less visible for the dynamically created wavepacket.

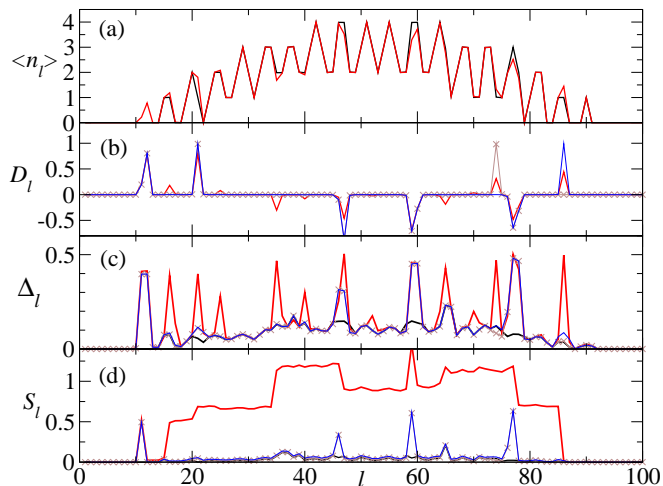


Figure 4: (color online) Same as fig. 2 but for $s_2 = 2.1875$. Here $r_0 = 0.1075$, $\phi = 0.0304$ in Eq.(2). Brown (blue) lines correspond to excitations X and Y in Fig. 1(c). The entanglement entropy is much larger for the dynamically created wavepacket than for stationary states, and Δ_l has many more peaks, indicating a significant melting of the Bose glass.

except in small SF pockets. Again, the wavepacket has different properties, with larger Δ_l and much larger entanglement entropy. The peaks in Δ_l are more numerous for the wavepacket than for the stationary states: they indicate melted regions.

In conclusion, we have built an extension of the TEBD algorithm capable of extracting, from the time-dependent wavefunction, important excited eigenstates populated

due to partially non-adiabatic dynamics, and the nature of the “defects” created. The properties of the excited states are essentially similar to that of the ground state even if the overlap of the wavepacket with the ground state is small. On the other hand, the dynamical wavepacket, as a linear combination of several excited states has a markedly different character. It reveals a significant entanglement across the whole sample.

It will be interesting to see how this picture is affected by temperature. On the one hand, finite temperature should lead to a decoherence of the entanglement. On the other hand, it probably destroys the Mott insulating character of the atomic sample even in deep lattices [18].

Support within Polish Government scientific funds for 2009-2012 as a research project is acknowledged. MŁ acknowledges support from Jagiellonian University International Ph.D Studies in Physics of Complex Systems (Agreement No. MPD/2009/6) provided by Foundation for Polish Science and cofinanced by the European Regional Development Fund. Computer simulations were performed at ACK Cyfronet AGH as a part of the POIG PL-Grid project (MŁ) and at ICM UW under Grant No. G29-10 (JZ and MŁ).

-
- [1] D. Jaksch et al., Phys. Rev. Lett. **81**, 3108 (1998).
 - [2] M.P.A. Fisher et al. Phys. Rev. B **40**, 546 (1989).
 - [3] M. Greiner et al., Nature **415**, 39 (2002).
 - [4] M. Lewenstein et al., Adv. Phys. **56**, 243 (2007).
 - [5] L. Fallani et al., Phys. Rev. Lett. **98**, 130404 (2007).
 - [6] M. White et al., Phys. Rev. Lett. **102**, 055301 (2009).
 - [7] J. Dziarmaga et al., Phys. Rev. Lett. **88**, 167001 (2002).
 - [8] A. Polkovnikov, Phys. Rev. B **72** 161201 (2005).
 - [9] J. Zakrzewski, Phys. Rev. A **71**, 043601 (2005); *ibid.* **72**, 039904 (2005).
 - [10] J. Zakrzewski and D. Delande, Phys. Rev. A **80**, 013602 (2009).
 - [11] E.E. Edwards et al., Phys. Rev. Lett. **101**, 260402 (2008).
 - [12] F. Gerbier et al., Phys. Rev. Lett. **95**, 050404 (2005); Phys. Rev. A **72**, 053606 (2005).
 - [13] J. F. Sherson et al., Nature **467**, 68 (2010).
 - [14] G. Vidal, Phys. Rev. Lett. **91**, 147902 (2003); *ibid.* **93**, 040502 (2004).
 - [15] M. Łański et al., in preparation.
 - [16] I. P. McCulloch, J. Stat. Mech.: Theory Exp. (2007) P10014.
 - [17] A. Kitaev and J. Preskill, Phys. Rev. Lett. **96**, 110404 (2006).
 - [18] F. Gerbier, Phys. Rev. Lett. **99**, 120405 (2007).
 - [19] T. Roscilde, Phys. Rev. A **77**, 063605 (2008); G. Roux et al., Phys. Rev. A **78**, 023628 (2008); X. Deng et al., Phys. Rev. A **78**, 013625 (2008).
 - [20] Such a description assumes that interactions does not distort Wannier functions. This is not completely true, as discussed in e.g. J. Li et al., New J. Phys. **8**, 154 (2006). This may lead to modifications of the effective U by about 10%. Still, the method described here to extract properties of eigenstates remains valid.